Published in final edited form as:
Angew Chem Int Ed Engl. 2010 May 10; 49(21): 3649–3652. doi:10.1002/anie.201000329.

A left handed solution to peptide inhibition of the p53-MDM2 interaction**

Min Liu[†],
Institute of Human Virology, University of Maryland School of Medicine, 725 W. Lombard St., Baltimore, MD 21201 (USA)

The First Affiliated Hospital, Xi'an Jiaotong University, School of Medicine (China)

Marzena Pazgier[†],
Institute of Human Virology, University of Maryland School of Medicine, 725 W. Lombard St., Baltimore, MD 21201 (USA)

Changqing Li[†],
Institute of Human Virology, University of Maryland School of Medicine, 725 W. Lombard St., Baltimore, MD 21201 (USA)

Weirong Yuan,
Institute of Human Virology, University of Maryland School of Medicine, 725 W. Lombard St., Baltimore, MD 21201 (USA)

Chong Li, and
Institute of Human Virology, University of Maryland School of Medicine, 725 W. Lombard St., Baltimore, MD 21201 (USA)

Wuyuan Lu
Institute of Human Virology, University of Maryland School of Medicine, 725 W. Lombard St., Baltimore, MD 21201 (USA)

Wuyuan Lu: wlu@ihv.umaryland.edu

Abstract

**This work was supported in part by a Research Scholar Grant CDD112858 from the American Cancer Society and the National Institutes of Health Grants AI072732 and AI061482 (to W.L.).

Correspondence to: Wuyuan Lu, wlu@ihv.umaryland.edu.

[†]These authors contributed equally to this work.

Supporting information for this article is available on the WWW under http://www.angewandte.org or from the author.

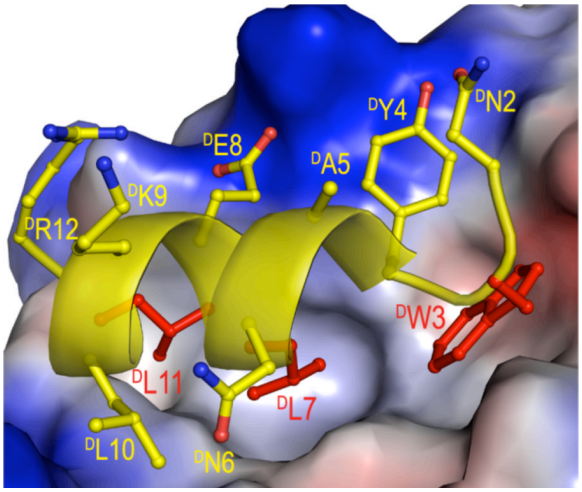

Throwing tumors a left hook punch: The oncoprotein MDM2 negatively regulates the activity and stability of the tumor suppressor protein p53, and is an important molecular target for anticancer therapy. Mirror image phage display identifies a high-affinity D-peptide ligand of MDM2 that can be developed into a potent and protease-resistant p53 activator with potential antitumor activity.

Keywords

p53; tumor suppressor; MDM2; D-peptides; drug discovery

Peptide inhibition of protein-protein interactions is a promising venue for the development of novel classes of therapeutic compounds[1]. Compared with small molecule inhibitors, peptides are capable of binding and antagonizing target proteins often with high affinity and unsurpassed specificity[2]. Despite significant progress in peptidomimetic chemistry and drug delivery, however, two major technical hurdles still hinder the thriving of peptide therapeutics – poor *in vivo* stability and membrane permeability. Here, we report the design, aided by mirror image phage display (MIPD)[3] and native chemical ligation (NCL)[4] of a potent D-peptide ligand, termed ^{D}PMI-β (TAWYANFEKLLR), of MDM2 – the oncogenic E3 ubiquitin ligase that negatively regulates the activity and stability of the tumor suppressor protein p53. Structural and functional studies indicate ^{D}PMI-β competes with p53 for MDM2 binding. Since inhibitors of the p53-MDM2 interaction activate the p53 signaling pathway and induce p53-dependent killing of tumor cells both *in vitro* and *in vivo*[5], the proteolytically stable ^{D}PMI-β and its derivatives, when coupled with a clinically viable delivery modality, may be of important therapeutic value in tumor eradication.

MDM2 binds the N-terminal transactivation domain of p53 to suppress p53-mediated growth inhibitory and apoptotic responses and to target p53 into the ubiquitin-proteasome pathway for degradation[6]. MDM2 recognizes a minimum of eight amino acid residues of p53, i.e., $F^{19}S^{20}D^{21}L^{22}W^{23}K^{24}L^{25}L^{26}$ [7], of which Phe19, Trp23 and Leu26 are the most critical residues for recognition[8]. By screening a phage-expressed duodecimal peptide library against a chemically synthesized, site-specifically biotinylated p53-binding domain of MDM2 ($^{25–109}$MDM2), we previously identified a potent L-peptide ligand termed PMI (TSFAEYWNLLSP) that bound MDM2 identically to p53 but at a significantly higher affinity ($K_d^{PMI\text{-}MDM2}$ = 3.2 nM)[9]. However, as L-peptides are susceptible to proteolytic degradation *in vivo* with poor bioavailability, PMI is of limited therapeutic value. To tackle peptide susceptibility to proteolysis, Kim and colleagues pioneered MIPD – an elegant

combinatorial technique that enables identification of proteolysis-resistant D-peptide ligands of a native protein through phage library screening against the (chemically synthesized) D-enantiomer of the L-target[3]. A broad application of MIPD in peptide drug discovery has been made possible by NCL – a powerful synthetic methodology for chemical protein synthesis developed by Kent and co-workers[4]. Screening the phage library against the D-enantiomer of $^{25–109}$MDM2 led to the identification of an L-peptide ligand of the D-protein - TNWYANLEKLLR (**Figure S1**). The D-enantiomer of this phage-selected peptide, termed ^{D}PMI-α, competed with p53 for MDM2 binding at an affinity of 219 nM (Table 1 and **Figure S2**) – 68-fold weaker than PMI but 2-fold stronger than $^{17–28}$p53 of the same length.

To decipher the structural basis of D-peptide inhibition of the p53-MDM2 interaction, we determined the co-crystal structure of ^{D}PMI-α and synthetic $^{25–109}$MDM2 at 2.4 Å resolution (**Table S1** and **Figure S3**). As shown in Figure 1A, ^{D}PMI-α adopts an amphipathic left-handed helical conformation in the complex, docking the hydrophobic side chains of ^{D}Trp3, ^{D}Leu7 and ^{D}Leu11 into the p53-binding cavity of MDM2. These three D-residues collectively contribute almost 60% of the total buried surface area (BSA) of ^{D}PMI-α in the complex. ^{D}Tyr4 forms π-cation interactions with Lys94 and stacks against His73 and Val93 of MDM2, while ^{D}Leu10 stabilizes the peptide-protein complex by making hydrophobic contacts with Leu54 and Phe55 (Figure 1B). Together, ^{D}Tyr4 and ^{D}Leu10 account for roughly 25% of the total BSA. Despite the dominance of hydrophobic force in ^{D}PMI-α and MDM2 recognition, electrostatic interactions also play an important role. Four H-bonds form between ^{D}PMI-α and MDM2, involving ^{D}Trp3 $N^{\varepsilon 1}$-Gln72 O, ^{D}Glu8 $O^{\varepsilon 1}$-Lys94 N^{ζ}, ^{D}Glu8 $O^{\varepsilon 2}$-His96 $N^{\varepsilon 2}$, and ^{D}Leu11 O-Ty100 O^{η}.

To verify the structural findings, we performed a ^{D}Ala scanning mutational analysis of ^{D}PMI-α at selective positions, and quantified the binding affinity of ^{D}PMI-α analogs for MDM2 using a surface plasmon resonance-based competiton assay[9, 10]. The K_d values are tabulated in Table 1 and individual binding curves presented in **Figure S2**. Four critical hydrophobic residues were identified, ^{D}Trp3, ^{D}Tyr4, ^{D}Leu7, and ^{D}Leu11, contributing 4.0, 2.2, 3.6, 2.3 kcal/mol, respectively, to ^{D}PMI-α binding to MDM2. A double mutation W3A/Y4A weakened the binding affinity of ^{D}PMI-α for MDM2 by over 2500-fold (4.6 kcal/mol). Interestingly, the N2A mutation improved ^{D}PMI-α activity by nearly a factor of 2, whereas the N6A mutation decreased the binding affinity by roughly 3-fold. Overall, the mutational data are concordant with the ^{D}PMI-α-MDM2 structure.

^{D}Trp3, ^{D}Leu7 and ^{D}Leu11 of ^{D}PMI-α are topologically equivalent to Phe3, Trp7, and Leu10 of PMI (or Phe19, Trp23, and Leu26 of p53) despite their opposite handedness (Figures 1C and 1D). Although the overall structures of peptide-bound MDM2 from the PMI-MDM2 and ^{D}PMI-α-MDM2 complexes are nearly identical (RMSD(C_α) = 0.56 Å) (**Figure S4**), superposition of MDM2 reveals notable structural differences at the binding interface between the two complexes. Unlike PMI, the N-terminus of ^{D}PMI-α is disordered with ^{D}Thr1 missing from and ^{D}Asn2 less well defined in the electron density map. The D-peptide shifts toward the α2 helix of MDM2, accompanied by a “close-in” movement of residues Val93 to Arg97 lining the opposite edge of the binding pocket. Consequently, Phe55 side chain flips outward to accommodate and interact with ^{D}Leu10, while the interacting pattern seen for Tyr6 of PMI is maintained for ^{D}Tyr4 of ^{D}PMI-α. In addition, two new H-bonds involving ^{D}Glu8 $O^{\varepsilon 1}$ and $O^{\varepsilon 2}$ form as indicated earlier. Finally, the side chain of Met62 and the main chain of Tyr67 recess to accommodate ^{D}Trp3 in the pocket that is occupied by the Phe residue of PMI or p53.

Importantly, ^{D}PMI-α binding to MDM2 did not induce any significant changes to the residues lining the bottom of the p53-binding pocket. As a result, the hydrophobic cavity

that accommodates Trp7 of PMI or Trp23 of p53 is only partially filled by the smaller ^{D}Leu7 side chain of ^{D}PMI-α, suggesting that functional improvement is possible through introduction of a bulkier hydrophobic residue to replace ^{D}Leu7. In fact, sequence analysis of all binding clones obtained from MIPD indicates that only Leu, Phe and Trp were selected at position 7 (**Figure S1**). We therefore mutated ^{D}Leu7 to ^{D}Phe and ^{D}Trp, and characterized L7F-^{D}PMI-α and L7W-^{D}PMI-α with respect to their binding to MDM2 (Table 1 and **Figure S2**). While the L7W mutation weakened ^{D}PMI-α binding (K_d increased to 352 nM), the L7F mutation enhanced the binding affinity of ^{D}PMI-α by almost 4-fold (K_d decreased to 59.8 nM). To further improve ^{D}PMI-α activity, a double mutation N2A/L7F was introduced, and the resultant D-peptide TAWYANFEKLLR, now termed ^{D}PMI-β, bound to MDM2 with a K_d value of 34.5 nM. The predicted ΔΔG value of −1.05 kcal/mol (−0.29–0.76) for ^{D}PMI-β relative to ^{D}PMI-α is in nearly perfect agreement with the measured binding free energy change of −1.08 kcal/mol due to strongly additive mutational effects. We also quantified ^{D}PMI-α and ^{D}PMI-β binding to MDMX – a homolog of MDM2 that non-redundantly abrogates the p53 signaling pathway[11]. Despite an almost 8-fold improvement in MDMX binding over ^{D}PMI-α, ^{D}PMI-β remains a weak ligand of MDMX (K_d = 2.4 μM) (**Figure S5**).

^{D}PMI-α and ^{D}PMI-β are fully resistant to proteolytic degradation (**Figure S6**). However, neither D-peptide is expected to actively traverse the cell membrane to exert p53-dependent tumor killing activity. Additional work needs to be done to develop delivery vehicles to ensure efficient cellular uptake of these D-peptide activators of p53. Particularly promising in this regard is the hydrocarbon stapling technique developed by Verdine and colleagues, which enables side-chain cross-linked L-α-helical peptides to actively permeabilize cells with enhanced biological activity and proteolytic stability[12]. Several hydrocarbon-stapled L-peptides with various *in vitro* and/or *in vivo* antitumor activities have been successfully designed, including a p53-activating peptide[1, 13]. It is conceivable that hydrocarbon stapling of the helical ^{D}PMI-α or ^{D}PMI-β should result in a cell-penetrating and p53-activating antitumor peptide with enhanced efficacy *in vivo* due to its full resistance to proteolysis. Notably, various peptidomimetic approaches have been used to design protease-resistant MDM2 antagonists to emulate the activity of the p53 peptide[14]. Of particular interest is the cyclic β-hairpin template developed by Robinson and colleagues[15]. Structured peptide scaffolds have also been used to engineer p53-emulating miniature proteins to antagonize MDM2[10, 16]. However, they are still subject to *in vivo* degradation by proteases.

In conclusion, by using NCL and MIPD coupled with mutational analysis and rational design, we identified for the first time potent D-peptide ligands of MDM2. X-ray crystallographic studies elucidated the structural basis for high-affinity D-peptide inhibition of the p53-MDM2 interaction, and validated the mode of action of ^{D}PMI peptides as a novel class of p53 activators. D-peptide inhibitors are superior to many existing drug candidates in aspects such as potency, specificity, and particularly, *in vivo* stability. Coupled with a therapeutically viable delivery modality, ^{D}PMI-α or ^{D}PMI-β and its derivatives may have the potential to be developed into antitumor agents for clinical use.

Experimental Section

Synthesis of D-peptides and D- and L-proteins

All peptides and proteins used in this work were chemically synthesized using the published protocols[4, 17]. MBHA resin was used for the synthesis of D-peptides/proteins, whereas L-peptides/proteins were made on PAM resins. The synthesis of $^{25–109}$MDM2, $^{24–108}$MDMX and N79K-biotin-L-$^{25–109}$MDM2 was described previously[9]. Identical procedures were used for the preparation of N79K-biotin-D-$^{25–109}$MDM2 (**Figures S7–S8**). All peptides and

proteins were purified to homogeneity by reversed-phase HPLC, and their molecular masses were ascertained by electrospray ionization mass spectrometry. Peptide and protein quantification was performed by UV measurements at 280 nm using molar extinction coefficients calculated according to the published algorithm[18].

Mirror image phage display

Screening of the Ph.D.-12™ duodecimal peptide phage library was carried out against 1 μM N79K-biotin-D-$^{25–109}$MDM2 immobilized on streptavidin-agarose resin as described[9]. Bound phage particles were competitively eluted with 1 mM D-$^{15–29}$p53, and subsequently amplified in host strain *E. coli* ER2738. After four rounds of selection, 10 binding clones were randomly picked and sequenced. A second independent screening was performed for confirmation (**Figure S1**).

Surface plasmon resonance based competition binding assay

The K_d values of D-peptides for MDM2 and MDMX were determined as described[9, 10]. A more detailed description of the assay conditions and the binding curves are presented as supplementary information (**Figure S2** and **Figure S5**). The results tabulated in Table 1 were from three independent measurements.

Crystallization, data collection, structure solution, and refinement

^{D}PMI-α-MDM2 crystals were grown at room temperature using the hanging-drop vapor diffusion method in a buffer containing 0.2 M ammonium sulfate, 0.1 M sodium cacodylate trihydrate, and 30% PEG 8000, pH 6.5. X-ray diffraction data were collected at the X-ray Crystallography Core Facility, University of Maryland at Baltimore. Data integration and scaling, and structure solution and refinement were performed as described[9]. $^{25–109}$MDM2 coordinates extracted from the MDM2-PMI complex structure (PDB code: 3EQS)[9] were used as a search model for molecular replacement. Data collection and refinement statistics are summarized in **Table S1**. Coordinates and structure factors have been deposited in the Protein Data Bank with accession number 3LNJ. Molecular graphics were generated using Pymol (http://pymol.org).

References

1. a) Moellering RE, Cornejo M, Davis TN, Del Bianco C, Aster JC, Blacklow SC, Kung AL, Gilliland DG, Verdine GL, Bradner JE. Nature. 2009; 462:182. [PubMed: 19907488] b) Walensky LD, Kung AL, Escher I, Malia TJ, Barbuto S, Wright RD, Wagner G, Verdine GL, Korsmeyer SJ. Science. 2004; 305:1466. [PubMed: 15353804]
2. Arkin MR, Wells JA. Nat Rev Drug Discov. 2004; 3:301. [PubMed: 15060526]
3. a) Schumacher TN, Mayr LM, Minor DL Jr, Milhollen MA, Burgess MW, Kim PS. Science. 1996; 271:1854. [PubMed: 8596952] b) Eckert DM, Malashkevich VN, Hong LH, Carr PA, Kim PS. Cell. 1999; 99:103. [PubMed: 10520998]
4. a) Dawson PE, Muir TW, Clark-Lewis I, Kent SB. Science. 1994; 266:776. [PubMed: 7973629] b) Kent SB. Chem Soc Rev. 2009; 38:338. [PubMed: 19169452]
5. a) Brown CJ, Lain S, Verma CS, Fersht AR, Lane DP. Nat Rev Cancer. 2009; 9:862. [PubMed: 19935675] b) Shangary S, Qin D, McEachern D, Liu M, Miller RS, Qiu S, Nikolovska-Coleska Z, Ding K, Wang G, Chen J, Bernard D, Zhang J, Lu Y, Gu Q, Shah RB, Pienta KJ, Ling X, Kang S, Guo M, Sun Y, Yang D, Wang S. Proc Natl Acad Sci U S A. 2008; 105:3933. [PubMed: 18316739] c) Vassilev LT, Vu BT, Graves B, Carvajal D, Podlaski F, Filipovic Z, Kong N, Kammlott U, Lukacs C, Klein C, Fotouhi N, Liu EA. Science. 2004; 303:844. [PubMed: 14704432]
6. a) Vousden KH, Lane DP. Nat Rev Mol Cell Biol. 2007; 8:275. [PubMed: 17380161] b) Toledo F, Wahl GM. Nat Rev Cancer. 2006; 6:909. [PubMed: 17128209]

7. Kussie PH, Gorina S, Marechal V, Elenbaas B, Moreau J, Levine AJ, Pavletich NP. Science. 1996; 274:948. [PubMed: 8875929] b) Schon O, Friedler A, Bycroft M, Freund SM, Fersht AR. J Mol Biol. 2002; 323:491. [PubMed: 12381304]
8. Bottger A, Bottger V, Garcia-Echeverria C, Chene P, Hochkeppel HK, Sampson W, Ang K, Howard SF, Picksley SM, Lane DP. J Mol Biol. 1997; 269:744. [PubMed: 9223638]
9. Pazgier M, Liu M, Zou G, Yuan W, Li C, Li J, Monbo J, Zella D, Tarasov SG, Lu W. Proc Natl Acad Sci U S A. 2009; 106:4665. [PubMed: 19255450]
10. Li C, Pazgier M, Liu M, Lu WY, Lu W. Angew Chem Int Ed Engl. 2009; 48:8712. [PubMed: 19827079]
11. Marine JC, Dyer MA, Jochemsen AG. J Cell Sci. 2007; 120:371. [PubMed: 17251377]
12. Schafmeister CE, Po J, Verdine GL. J Am Chem Soc. 2000; 122:5891.
13. Bernal F, Tyler AF, Korsmeyer SJ, Walensky LD, Verdine GL. J Am Chem Soc. 2007; 129:2456. [PubMed: 17284038]
14. Murray JK, Gellman SH. Biopolymers. 2007; 88:657. [PubMed: 17427181]
15. a) Fasan R, Dias RL, Moehle K, Zerbe O, Vrijbloed JW, Obrecht D, Robinson JA. Angew Chem Int Ed Engl. 2004; 43:2109. [PubMed: 15083458] b) Robinson JA. Acc Chem Res. 2008; 41:1278. [PubMed: 18412373]
16. a) Kritzer JA, Zutshi R, Cheah M, Ran FA, Webman R, Wongjirad TM, Schepartz A. Chembiochem. 2006; 7:29. [PubMed: 16397877] b) Hu B, Gilkes DM, Chen J. Cancer Res. 2007; 67:8810. [PubMed: 17875722] c) Li C, Liu M, Monbo J, Zou G, Yuan W, Zella D, Lu WY, Lu W. J Am Chem Soc. 2008; 130:13546. [PubMed: 18798622]
17. Schnolzer M, Alewood P, Jones A, Alewood D, Kent SB. Int J Pept Protein Res. 1992; 40:180. [PubMed: 1478777]
18. Pace CN, Vajdos F, Fee L, Grimsley G, Gray T. Protein Sci. 1995; 4:2411. [PubMed: 8563639]

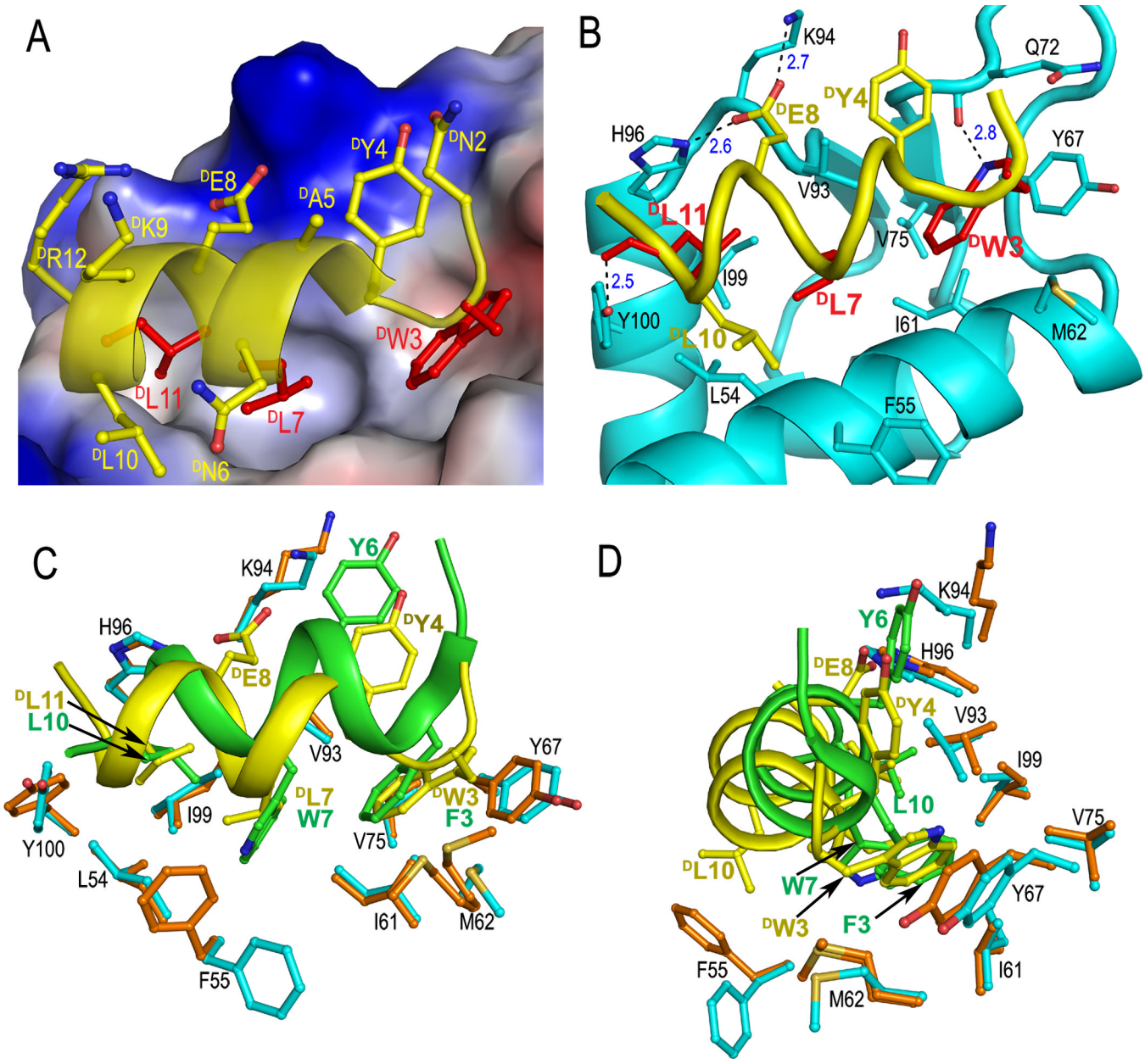

Figure 1.

Co-crystal structure of ^{D}PMI-α and $^{25–109}$MDM2. (**A**) Close-up view of the interface of the ^{D}PMI-α-MDM2 complex. The side chains of ^{D}Trp3, ^{D}Leu7, and ^{D}Leu11 of ^{D}PMI-α are colored in red, the rest in yellow. The electrostatic potential at the molecular surface of MDM2 is displayed as negative in red, positive in blue, and apolar in white. (**B**) A ribbon and stick representation of the binding interface. Only the side chains involved in direct interactions between ^{D}PMI-α (yellow) and MDM2 (cyan) are shown in sticks. The dash lines depict inter-molecular H-bonds. (**C**) ^{D}PMI-α(yellow) and PMI (green) from their respective complexes with (superimposed) MDM2. Residues lining the hydrophobic cavity of MDM2 are shown as orange sticks in the PMI complex and cyan sticks in the ^{D}PMI-α complex. (**D**) The side view of (C) after a 90° rotation.

Table 1

Amino acid sequences of PMI, $^{17–28}$p53, ^{D}PMI-α, ^{D}PMI-α analogs, and ^{D}PMI-β and their dissociation equilibrium constants (K_d) for synthetic $^{25–109}$MDM2. Each K_d value is the mean of three independent measurements.

Name	Sequence	K_d ± S.D. (nM)	ΔΔG (kcal/mol)
PMI	TSFAEYWNLLSP	3.2*	N.A.
$^{17–28}$p53	ETFSDLWKLLPE	452*	N.A.
^{D}PMI-α	TNWYANLEKLLR	219 ± 11	0
N2A-^{D}PMI-α	T**A**WYANLEKLLR	134 ± 6	−0.29
W3A-^{D}PMI-α	TN**A**YANLEKLLR	197 ± 10 μM	3.96
Y4A-^{D}PMI-α	TNW**A**ANLEKLLR	9.4 ± 0.6 μM	2.19
W3A/Y4A-^{D}PMI-α	TN**AA**ANLEKLLR	558 ± 30 μM	4.57
N6A-^{D}PMI-α	TNWYA**A**LEKLLR	730 ± 40	0.70
L7A-^{D}PMI-α	TNWYAN**A**EKLLR	108 ± 6 μM	3.61
E8A-^{D}PMI-α	TNWYANL**A**KLLR	2.3 ± 0.1 μM	1.37
L10A-^{D}PMI-α	TNWYANLEK**A**LR	982 ± 52	0.87
L11A-^{D}PMI-α	TNWYANLEKL**A**R	10.7 ± 0.5 μM	2.27
L7F-^{D}PMI-α	TNWYAN**F**EKLLR	59.8 ± 5.9	−0.76
L7W-^{D}PMI-α	TNWYAN**W**EKLLR	352 ± 24	0.28
^{D}PMI-β	T**A**WYAN**F**EKLLR	34.5 ± 0.6	−1.08

*The K_d values of PMI and $^{17–28}$p53 were from[9, 10], but determined under identical conditions.